ACS APPLIED MATERIALS & INTERFACES

Research Article

www.acsami.org

Delivery of Mitogen-Activated Protein Kinase Inhibitor for Hepatocellular Carcinoma Stem Cell Therapy

Yang Liu,[†] Xin Wang,[†] Chun-Yang Sun,[†] and Jun Wang*[,†,‡,§]

[†]The CAS Key Laboratory of Innate Immunity and Chronic Disease, School of Life Sciences and Medical Center, University of Science & Technology of China, Hefei, Anhui 230027, China

[‡]Hefei National Laboratory for Physical Sciences at Microscale, Hefei, Anhui 230027, China

[§]High Magnetic Field Laboratory of CAS, University of Science and Technology of China, Hefei, Anhui 230026, China

Supporting Information

ABSTRACT: Hepatocellular carcinoma (HCC) is one of the most common malignant human tumors worldwide, but no effective therapeutic options are currently available. The cancer stem cell (CSC) has proven to play a central role in the development, metastasis, and recurrence of HCC. In this study, we report a dual functional mitogen-activated protein kinase inhibitor (U0126)-based therapy for treating both bulk HCC and HCC CSCs, using poly(ethylene glycol)-*b*-poly(*d*,*l*-lactide) (PEG-PLA) nanoparticles as the drug carrier. It is demonstrated that nanoparticle encapsulation enhanced the cell uptake of U0126 in HCC CSCs and that enhanced endocytosis lead to augmented cytotoxicity of U0126 in HCC CSCs. Moreover, the nanoparticle encapsulation increased the inhibition of self-renewal capability, prolonged the circulation time, and increased the tumor accumulation of U0126 when compared with the use of the free inhibitor. The systemic delivery of U0126 remarkably enhanced the suppression of tumor development with decreased CSCs in the HepG2 xenograft simultaneously with reduced systemic toxicity.

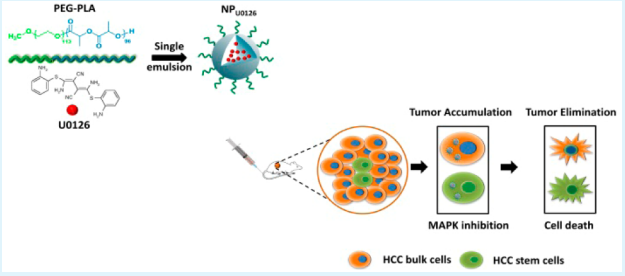

KEYWORDS: *hepatocellular carcinoma, CSC, mitogen-activated protein kinase, U0126, nanoparticle*

INTRODUCTION

Hepatocellular carcinoma (HCC) is usually diagnosed at an advanced stage, and thus, the most commonly used therapies such as resection, transplantation, or percutaneous lack efficacy.[1] Moreover, HCC is resistant to the conventional chemotherapy and barely amenable to radiotherapy, leaving no therapeutic options and a bad prognosis.[2,3] Recently, more attention has been paid to the HCC cancer stem cells (CSC) concept in the design of anticancer drugs.[4] CSCs in hepatocellular carcinoma evade the anticancer effects of standard chemotherapy[5,6] or radiotherapy,[7] emerging as an underestimated biological barrier to the success of systemic chemotherapy. Suetsugu et al. first demonstrated that the CD133 positive subpopulation of HCC possesses CSC-like properties,[8] and the high capacity for tumorigenicity of CD133-positive HCC was further proved by Yin et al.[9] Moreover, the CSC percentage was found to be relative to the prognosis and overall survival in patients suffering from HCC.[10−12] Therefore, CSC-related therapy may provide an approach for cancer therapy[13−16] and for HCC.

More recently, Zhao et al. found that the mitogen-activated protein kinase (MAPK) pathway could regulate the liver tumor initiation capacity.[17] The MAPK pathway is a mitogenic cascade,[18] and the intermediate in this pathway is extracellular-regulated kinase (ERK1/2).[19] The MAPK pathway is proved a key regulatory pathway for control points such as cell survival, migration and transformation in various types of tumor including HCC.[20−22] A previous study proved the importance of MAPK in HCC cell proliferation and the inhibition of this pathway could affect the cell proliferation and apoptosis in HCC.[23] Zhao et al. proved that this pathway could also affect the cancer stem cell properties of HCC,[17] and as several recent works reported, the MAPK pathway also played key role in the maintain of stemness, and self-renewal in various types of cancer stem cell such as breast cancer, glioblastoma cells, and chronic myeloid leukemia.[24−26] Combining the important role of the MAPK pathway in HCC CSCs with the proven cytotoxicity of MAPK inhibition in the bulk HCC, we consider that inhibition of the MAPK signaling pathway might eliminate both the bulk HCC and rare CSCs.

The most widely used MAPK inhibitor, U0126, is a hydrophobic compound[27] and may encounter barriers in clinical use, such as the degradation of therapeutics in blood, rapid clearance by the immune system, glomerular filtration and excretion, and cellular barriers.[28−30] Nanoparticle-mediated delivery of chemotherapeutic agents has been demonstrated

Received: November 25, 2014
Accepted: December 18, 2014
Published: December 18, 2014

DOI: 10.1021/am508262j
ACS Appl. Mater. Interfaces 2015, 7, 1012−1020

Scheme 1. Schematic Illustration of Nanoparticles Preparation and Suppression of Tumor by Eliminating Both CSCs and Non-CSCs

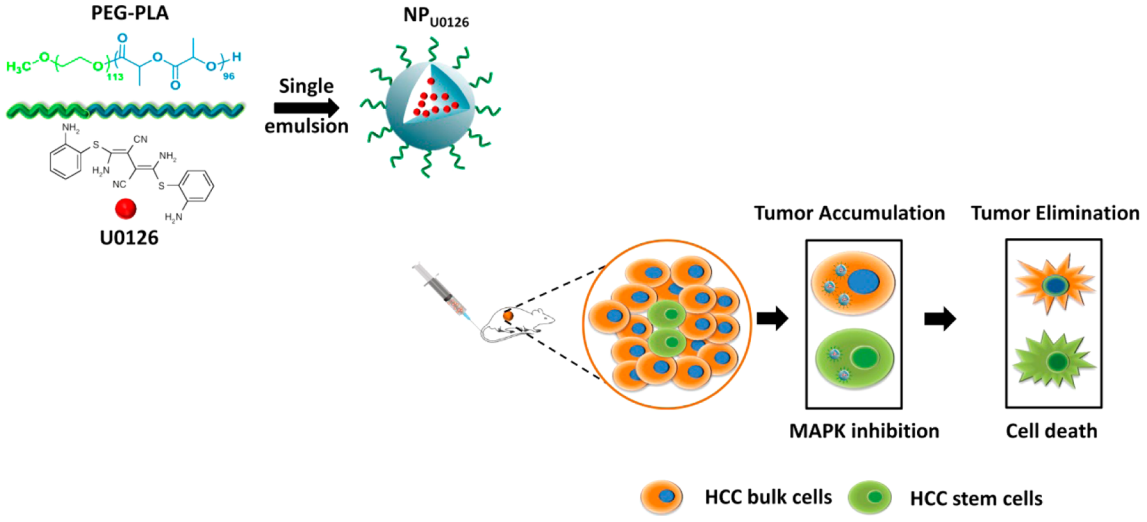

to overcome the biological and physiological barriers mentioned above, and enhanced anticancer efficacy has been achieved with reduced side effects in cancer prevention and treatment.[31−38] In particular, nanoparticles with the proper structures, sizes, and surface properties would readily accumulate and be retained in solid tumors because of the enhanced permeability and retention (EPR) effect.[39−43] Recently, studies of nanoparticle delivery system-based approaches to tackle the CSC problem have been reported.[44,45] Herein, we address a promising strategy involving the delivery of the MAPK inhibitor with nanoparticles prepared by a single emulsion method for both HCC CSCs and bulk HCC inhibition (Scheme 1). The drug-loaded nanoparticles (NP$_{U0126}$) could effectively increase cellular uptake of the inhibitor, especially in HCC CSCs. Treatment with NP$_{U0126}$ attenuates the tumor initiating ability and eventually enhances the cytotoxicity in HCC CSCs. Furthermore, intravenous administration of the nanoparticles apparently prolongs the circulation time and increases enrichment of the drug in tumor tissue. Systemic delivery of U0126 remarkably enhances the suppression of tumor growth and decreases the CSCs in HepG2 xenograft simultaneously with reduced systemic toxicity.

EXPERIMENTAL SECTION

Materials. Poly(ethylene glycol)-*block*-poly(*d,l*-lactide) (PEG$_{5K}$-PLA$_{11K}$) was synthesized and purified according to a previously reported procedure.[43] Insulin, dimethyl sulfoxide (DMSO), and methyl thiazol tetrazolium (MTT) were obtained from Sigma-Aldrich (St. Louis, MO). Fetal bovine serum (FBS) was purchased from Excell Bio (Shanghai, China). Dulbecco's modified Eagle's medium (DMEM), Dulbecco's modified Eagle's medium/nutrient mixture F-12 (DMEM/F-12) medium, Roswell Park Memorial Institute (RPMI) 1640 medium, B27 and recombinant human epidermal growth factor (hEGF) were obtained from Invitrogen (Carlsbad, CA). Basic fibroblast growth factor (bFGF) and hepatocyte growth factor (HGF) were purchased from Peprotech (Rocky Hill, NJ).

Cell Culture. HCC cell lines HepG2, Hep3B (American Type Culture Collection, Manassas, VA), and SMMC-7721 (Type Culture Collection of the Chinese Academy of Sciences, Shanghai, China) were maintained in DMEM with 10% FBS. For sphere formation, the serum-free DMEM-F12, supplemented with B27, 20 ng/mL hEGF, 20 ng/mL bFGF, 10 ng/mL HGF, 0.4% bovine serum albumin (BSA, Sangon Biotech, Shanghai, China), and 4 mg/mL insulin was used for the suspended culture of HCC at the concentration of 1000 cells/mL.

MEK/ERK Inhibitor. U0126 (Selleck Chemicals, Houston, TX) was reconstituted in DMSO for the in vitro use. Hydroxypropyl cyclodextrin (HPBCD, 20%, Aladdin, Shanghai, China) was used for the reconstitution of the inhibitor for animal studies.

Preparation and Characterization of Nanoparticles with Drug Encapsulation. Nanoparticles encapsulated with U0126 (denoted as NP$_{U0126}$) were prepared by a single emulsion-solvent evaporation technique. Briefly, a solution of U0126 (1 mg), and PEG$_{5K}$-PLA$_{11K}$ (25 mg) in 0.5 mL of ethyl acetate was emulsified in 4 mL of ultrapurified water by sonication (Sonics & Materials, Newtown, CT) for 60 s over an ice bath. The mixture was added to a 50 mL round-bottom flask, and the solvent was concentrated under reduced pressure by a rotary vacuum evaporator to a volume of 1 mL. The unencapsulated drug was purified by centrifugation (1000*g*, 15 min). Zeta potentials and particle size measurements were conducted following a previously reported procedure.[37] The nanoparticles were incubated in DMEM with 10% FBS (v/v) at 37 °C for 6 days for the stability study. The change of the particle size is monitored at interval time.

High-performance liquid chromatography (HPLC) was used for the evaluation of encapsulation efficiency of U0126 in the formulation. HPLC using a Waters HPLC system consisting of a Waters 1525 binary pump, a Waters 2487 absorbance detector, a 1500 column heater, and a Symmetry C18 column was used to measure the concentration of U0126. Methanol with H_2O at a ratio of 60:40 (v/v) was used as the mobile phase. The absorbance detector was set to 245 nm. The encapsulation efficiency U0126 was calculated similar to a previously reported study.[46]

In Vitro Release of U0126. The U0126-loaded nanoparticles were incubated in different buffers (phosphate buffer, PB, 0.02 M, pH 7.4; acetate buffer solution, 0.02 M, pH 5.0) at 37 °C. After specific time intervals, the absorption spectra was measured. To determine the cumulative release behavior of nanoparticles, the solutions were transferred to a dialysis tube (MWCO 3400 Da) and immersed in 15 mL of the corresponding buffer in a shaker at a temperature of 37 °C. The external solutions (2% HPBCD in the above buffers) were collected and replaced by fresh buffers at the predetermined time. The collected solutions were freeze-dried, and the concentration of U0126 was measured by HPLC.

Cellular Uptake. HepG2, Hep3B, or SMMC-7721 adherent cells or mammosphere cells (5×10^4) were seeded and cultured for 1 day before incubation with NP$_{U0126}$. The cells were incubated at 37 °C with NP$_{U0126}$ suspended in complete culture medium at a concentration of 10 μM. Free U0126 (10 μM, in DMSO) was

DOI: 10.1021/am508262j
ACS Appl. Mater. Interfaces 2015, 7, 1012−1020

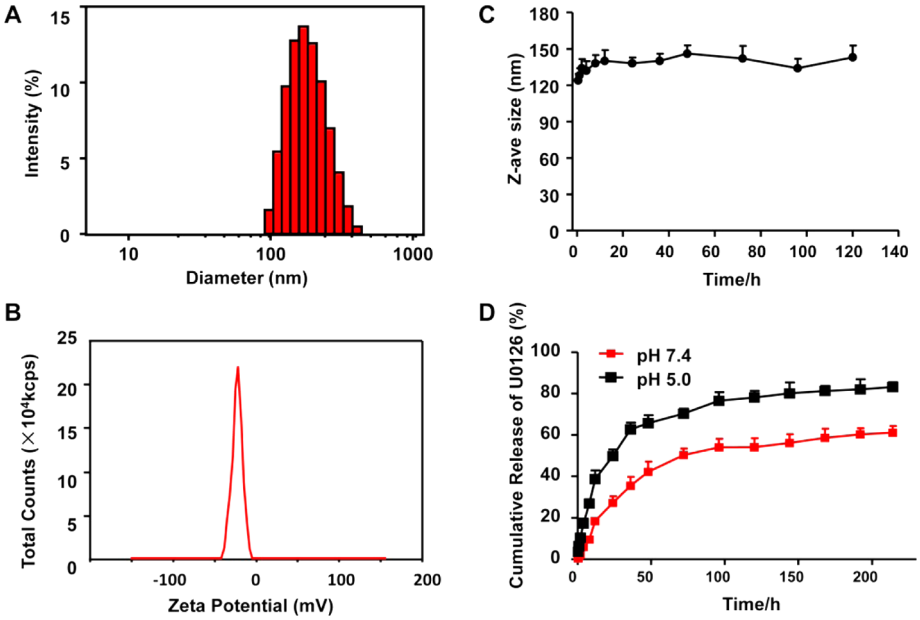

Figure 1. Characterization of U0126-loaded nanoparticles. (A) Size and (B) zeta potential determined by the DLS. (C) Stability and (D) drug release profiles of U0126-loaded nanoparticles.

added as a control. Four hours later, the cells were typsinized by Trypsin-EDTA solution (Invitrogen, Carlsbad, CA) and washed with PBS. After centrifugation at 1500*g* for 20 min, cell precipitation was dissolved in 100 μL DMSO and further analyzed by HPLC. The cell numbers of each group were used for normalization.

Cytotoxicity of U0126-Loaded Nanoparticles in Vitro. The cell proliferation with U0126 treatment was assessed by MTT viability assay in HepG2, Hep3B, and SMMC-7721 adherent or mammosphere cells. For the adherent cell lines, cells at a concentration of 5000 cells per well were seeded in 96-well plates. Mammosphere cells at concentration of 10 000 cells per well were seeded in ultralow adhesion 96-well plates. Then, NP, NP_{U0126}, or free U0126 at various concentrations was added and incubated for another 72 h. The MTT assay was then proceeded as described previously.[15]

Mammosphere Formation and CSC Ratios Assay after Drug-Loaded Nanoparticles Treatment in Vitro. HepG2, Hep3B, and SMMC-7721 mammosphere cells were treated with equivalent U0126 or NP_{U0126} doses of 5 μM for 4 h. For mammosphere formation assay, the cells were then washed with PBS. Next, 1,000 cells were plated per well in ultralow adhesion 24-well plates (n = 96) and cultured for 14 days prior to being counted. For determination of the CSC ratios, cells were collected and stained with CD133-PE or isotype control antibody (IgG-PE) (Miltenyi Biotec, Shanghai, China) for 30 min at 37 °C and then acquired using a FACS Calibur flow cytometer (Becton Dickinson, Franklin Lakes, NJ) and analyzed by FlowJo Software, with the isotype control antibody-stained population used as a negative control.

In Vitro Limiting Dilution Assays. HepG2, Hep3B, and SMMC-7721 mammosphere cells were treated with equivalent U0126 or NP_{U0126} doses of 5 μM for 4 h. The mammosphere cells were collected and serially diluted from 128 to 2 cells per well (n = 10) in the ultralow attachment 96-well culture plates with complete mammosphere medium. After 14 days, those colonies containing more than 10 cells were counted under the microscope. The Extreme Limiting Dilution Analysis software was detailed parameters calculation.[47]

Pharmacokinetics Studies. Free U0126 or NP_{U0126} was injected into imprinting control region (ICR) mice (Beijing HFK Biotechnology Co., Ltd., Beijing, China) intravenously (iv) at a dose of 10 mg/kg. Blood samples were collected at a predetermined time point. The blood was then centrifuged at 4 °C (3000 g, 10 min) to collect the plasma. To extract U0126 from the plasma, we mixed 200 μL of acetonitrile with 100 μL of plasma and allowed the mixture to stand at room temperature for 15 min. The resultant mixture was further extracted with chloroform (800 μL). The organic solution containing U0126 which was obtained after centrifugation at 10 000*g* for 10 min was collected and dried. The content of U0126 was then analyzed by HPLC according to the method as previously described.[48]

Drug Biodistribution. Free U0126 or NP_{U0126} was administered intravenously into nude mouse (Beijing HFK Biotechnology Co. Ltd., Beijing, China) bearing a HepG2 tumor at 10 mg per kg of body weight. Six hours later, the major organs and tumor were excised, washed, dried, and weighed. The tissues were homogenized and 200 μL (10%, w/v) of tissue homogenate was exposed to 200 μL of acetonitrile for 10 min. The resultant mixture was further extracted with chloroform (800 μL). The organic solution containing U0126, which was obtained after centrifugation at 10 000*g* for 10 min, was collected and dried. The content of U0126 was analyzed by HPLC as described above.

Human Hepatocellular Carcinoma Cancer Xenograft Tumor Model and Tumor Suppression Study. Female Nonobese Diabetic/Severe Combined Immunodeficiency (NOD/SCID) mice (8 weeks old) were purchased from Beijing HFK Biotechnology Co., Ltd. (Beijing, China), and all animals received care in compliance with the guidelines outlined in the Guide for the Care and Use of Laboratory Animals. The procedures were approved by the University of Science and Technology of China Animal Care and Use Committee.

The tumor models were generated by the subcutaneous injection of 100 μL HepG2 cells (5×10^6 per mouse) on the backs of the mice. When tumor volume was about 50 mm^3, the mice were randomly divided and treated by iv injection of PBS, free U0126, or NP_{U0126} at 10 mg/kg twice a week for 4 weeks. The tumor volume was calculated as followed formula: tumor volume = $1/2 \times \text{width}^2 \times \text{length}$.

Analysis of the Ratio of CSCs in Tumor. One day after the last treatment, the animals were sacrificed, and tumor tissues were excised. The tumor cells were collected according to the method reported before.[49] The cells were stained with CD133-PE or IgG-PE, as described above, and analyzed by FACS Calibur flow cytometer.

Tumor Immunohistochemical Analysis and Mouse Cytokine Analysis. Twenty-four hours after the last treatment, the tumor tissues and the mouse serum were collected. The tissues were fixed in 4% formaldehyde and embedded in paraffin for analysis. The proliferation and apoptosis of tumor cells and the AST, ALT, and LDH levels in the mouse serum were analyzed as previously reported.[50]

DOI: 10.1021/am508262j
ACS Appl. Mater. Interfaces 2015, 7, 1012−1020

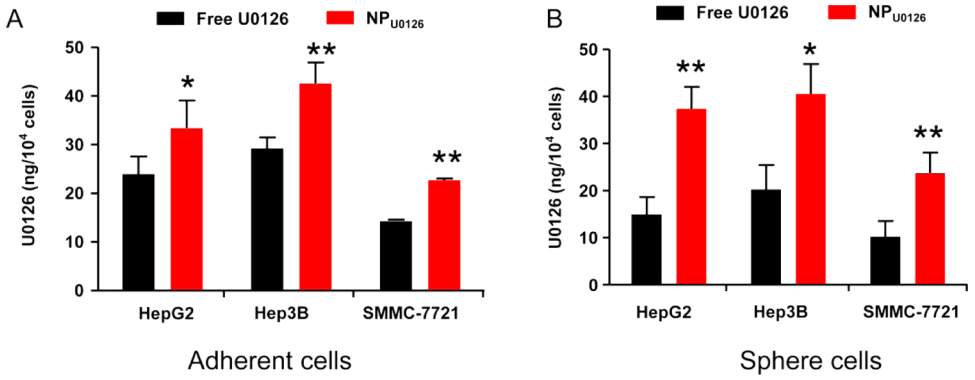

Figure 2. Nanoparticles significantly increase cellular uptake of U0126 in vitro. HPLC analyses of intracellular U0126 concentrations in (A) HCC adherent cells and (B) CD133-positive HCC mammosphere cells after 4 h of treatment with different formulations. Data are shown as means ± SD (n = 3); (*) $p < 0.05$, (**) $p < 0.01$, NP$_{U0126}$ compared with free U0126 in each cell line.

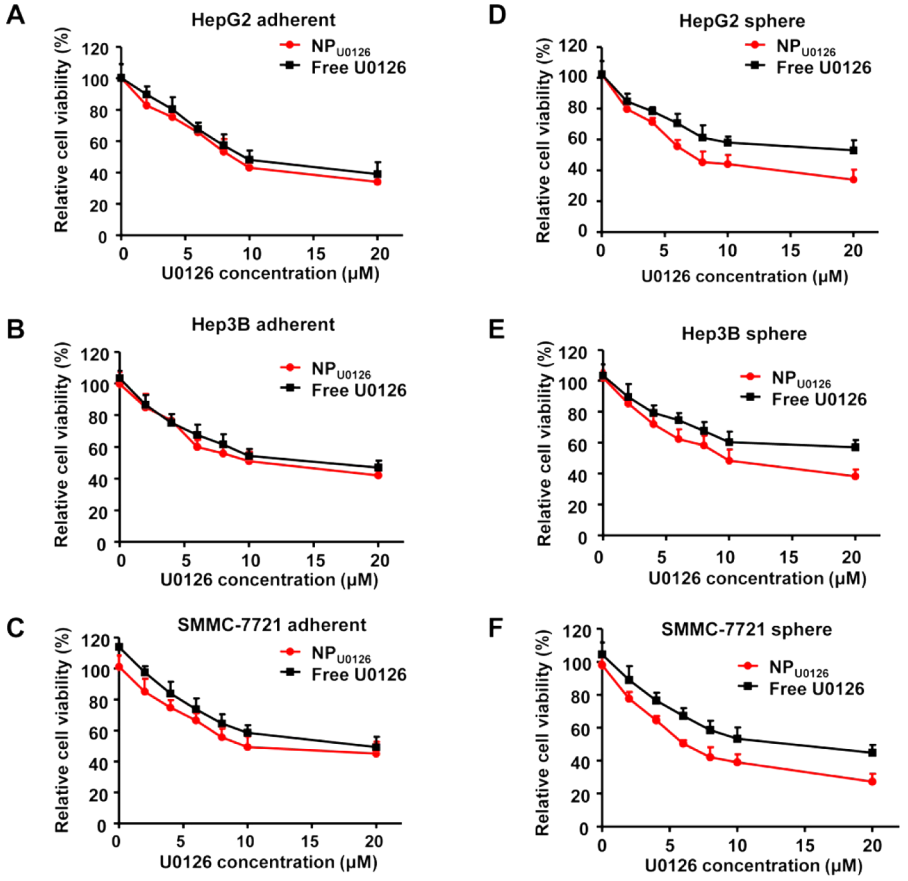

Figure 3. Cytotoxicity of free U0126 or NP$_{U0126}$ in (A−C) HepG2, Hep3B, SMMC-7721 adherent and (D−F) mammosphere cells. Data are shown as means ± SD (n = 6).

Statistical Analysis. The statistical significance was assessed using Student's t-test (two-tailed); $p < 0.05$ was considered statistically significant in all analyses (95% confidence level).

RESULTS AND DISCUSSION

Preparation and Characterization of Nanoparticles with Drug Encapsulation. About 40% of active substances identified by combinatorial screening programs are proved highly hydrophobic.[51] Their bioavailabilities in the human body is limited by their poor solubilities and rapid uptake by the reticule-endothelial system (RES).[52] Nanotechnology has been utilized to overcome the limitations of poorly water-soluble compounds.[53] In this study, by using a biocompatible and biodegradable PEG$_{5K}$-PLA$_{11K}$ copolymer and single emulsion-solvent evaporation technique, we prepared drug-loaded nanoparticles donated as NP$_{U0126}$. The average particle size (129 ± 2.4 nm) and the zeta potential (−12.4 ± 1.7 mV) of the nanoparticles were determined by DLS (Figure 1A,B). Such drug-encapsulated nanoparticles exhibited high encapsulation efficiency of drug (70.1%) and a sufficient loading content of drugs (3.5%, w/w) that were precisely determined by HPLC. To demonstrate the stability of the prepared nanoparticles, NP$_{U0126}$ was incubated in 10% FBS at 37 °C, and the size changes were monitored by DLS measurements. As shown in

DOI: 10.1021/am508262j
ACS Appl. Mater. Interfaces 2015, 7, 1012−1020

Figure 1C, for up to 120 h, the diameters of the nanoparticles barely changed. The PEG blocks that are presented at the surface of nanoparticles can help prevent protein adsorption and the aggregation of nanoparticles.[54] Furthermore, we determined the drug release profile of U0126-loaded nanoparticles in release medium at pH 7.4 and 5.0 in order to mimic the extra- and intracellular environments, as shown in Figure 1D. NP_{U0126} exhibited sustained U0126 release at pH 7.4 (about 60% after 9 d), and an increased release (approximately 80% after 9 d) was observed at a lower pH. The amines within the structure of U0126 might augment the solubility of the hydrophobic U0126 in acid environments and contribute to the accelerated release of U0126 from nanoparticles encapsulation.

Delivery of U0126 to HCC Adherent Cells and HCC Mammosphere Cells by Drug-Loaded Nanoparticles. A serum-free and nonadherent cell culture method was employed for the enrichment of CSCs and the resulting mammospheres were used in the following experiments.[55] To demonstrate that nanoparticles can transport U0126 molecules into normal HCC cells and HCC CSCs, we used HepG2-, Hep3B-, and SMMC7721-adherent and mammospheres cells. After incubating with free U0126 or NP_{U0126} at 10 μM for 4 h, the U0126 content in HepG2, Hep3B, and SMMC7721 adherent cell lines was analyzed by HPLC and normalized against the cell numbers of each group. As shown in Figure 2A, the nanoparticles could enhance the cellular uptake of U0126 compared to free U0126 in all three cell lines, possibly due to the different endocytosis pathways between NP_{U0126} and free U0126. Moreover, NP_{U0126} could more efficiently deliver the drug into the previously reported drug-resistant mammosphere cells compared to free drug (Figure 2B). The drug contents in HCC mammosphere cells were lower than in HCC adherent cells after free U0126 treatment (adherent, HepG2 24.0, Hep3B 29.2, and SMMC7721 16.9 ng per 10^4 cells; mammosphere, HepG2 14.9, Hep3B 20.1 and SMMC7721 10.2 ng per 10^4 cells, respectively). However, the nanoparticles could facilitate cellular uptake of the drug in mammosphere cells and better function in the CSCs (free U0126, HepG2 14.9, Hep3B 20.1, and SMMC7721 10.2 ng per 10^4 cells; NP_{U0126}, HepG2 37.3, Hep3B 40.6, and SMMC7721 23.7 ng per 10^4 cells, respectively).

The Cytotoxicity and Self-Renewal Inhibition of NP_{U0126}. The MAPK pathway is a mitogenic signaling cascade and is a key regulatory enzyme in the cell cycle, apoptosis, and tumorigenicity in human HCC, as previously reported.[18] U0126 is a widely used MAPK small molecular inhibitor that inhibits the phosphorylation of ERK1,2. More recently, Zhao et al. reported that the MAPK pathway played a pivotal role in the stemness maintenance of HCC CSCs.[17] With U0126 treatment, the self-renewal capability of HCC CSCs was apparently reduced, and induced apoptosis of CSCs was observed. Thus, we next explored whether NP_{U0126} could inhibit the cell proliferation in both HCC adherent cells and CSC-enriched mammosphere cells. First, the cytotoxicity of the free PEG-PLA nanoparticles was examined in both HCC adherent cells and mammospheres. As shown in Figure S1 (Supporting Information), the free nanoparticles at concentration up to 1 mg/mL have no significant effect on the cell viabilities, showing its good biocompatibility with both adherent cells and mamosphere cells. As shown in Figure 3A–C, NP_{U0126} could induce a dose-dependent cell viability inhibition in HepG2, Hep3B, and SMMC-7721-adherent cell lines. A similar cell proliferation inhibition was demonstrated with free U0126 treatment. However, when it comes to the HCC mammosphere cells, NP_{U0126} showed its superiority over free U0126. As shown in Figure 3D, NP_{U0126} could induce about 65% cell inhibition at a dose of 20 μM, while free U0126 caused 48% cell viability inhibition at the same dose in HepG2 mammosphere cells. Similar results were demonstrated in the Hep3B and SMMC-7721 mammosphere cells, as shown in Figure 3E,F.

To prove that nanoparticles carrying U0126 could inhibit cancer initiation of HCC CSCs, we performed the sphere formation assay. After treatment with U0126 or NP_{U0126} (10 μM) for 4 h, HepG2, Hep3B, and SMMC-7721 mammosphere cells were collected and seeded into an ultralow adhesion 24-well plate with sphere medium. As shown in Figure 4A, NP_{U0126} could reduce the sphere formation rate from 16.5% in the control group to 3.7% in HepG2 mammosphere cells, which was lower than in cells treated with free U0126 (6.6%). A similar enhanced sphere formation inhibition of NP_{U0126} was

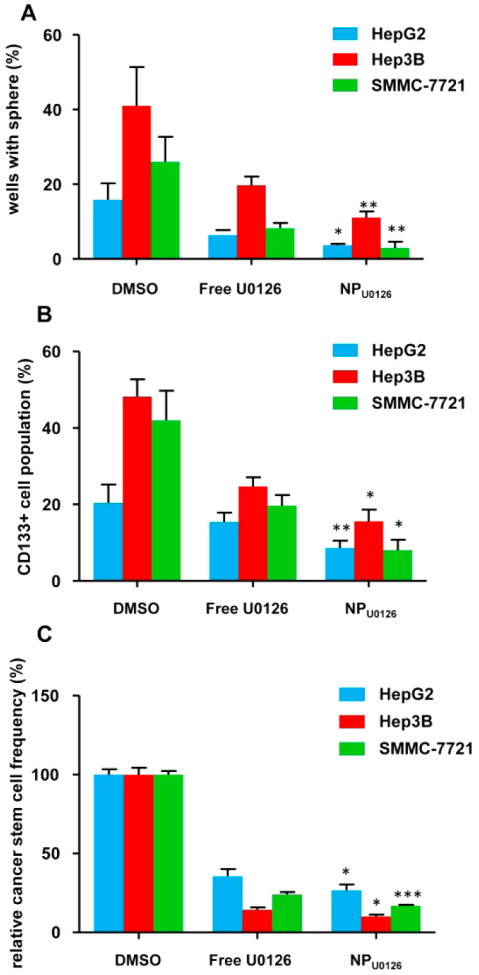

Figure 4. NP_{U0126} significantly inhibits self-renewal and affects the stemness of the CSCs. (A) The sphere formation assay in HCC mammosphere cells after 4 days of pretreatment with free U0126 or NP_{U0126}. (B) The proportion of CD133 positive cells in HCC mammosphere cells after 4 days of treatment with different formulations. (C) In vitro limiting dilution assays performed with HCC mammosphere cells on day 14 after pretreatment with different formulations for 4 h. The CSC frequency was calculated using Extreme Limiting Dilution Analysis software. Data are shown as means ± SD (n = 6). (*) $p < 0.05$, (**) $p < 0.01$, (***) $p < 0.001$, NP_{U0126} compared with free U0126 in each cell line.

DOI: 10.1021/am508262j
ACS Appl. Mater. Interfaces 2015, 7, 1012–1020

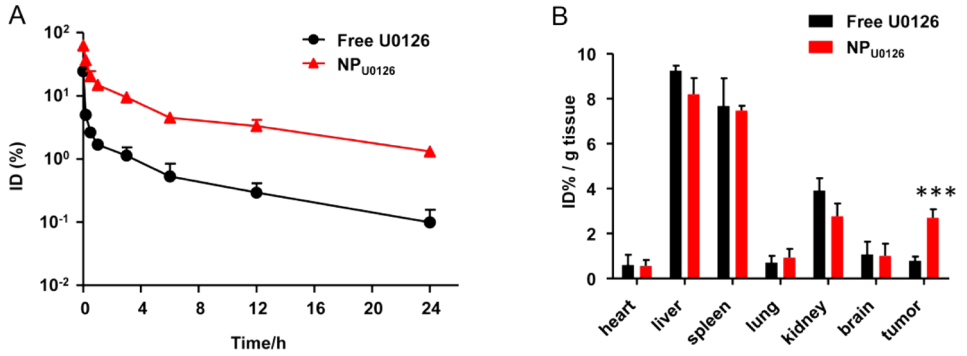

Figure 5. (A) Plasma U0126 concentration versus time after the intravenous administration of different formulations for 24 h at an equivalent dose of 10 mg per kg of mouse body. (B) HPLC analyses of the U0126 concentrations in HepG2 xenograft major organs and tumors 6 h after iv administration of different formulations. Data are shown as means ± SD (n = 3). (***) p < 0.001, NP$_{U0126}$ compared with free U0126.

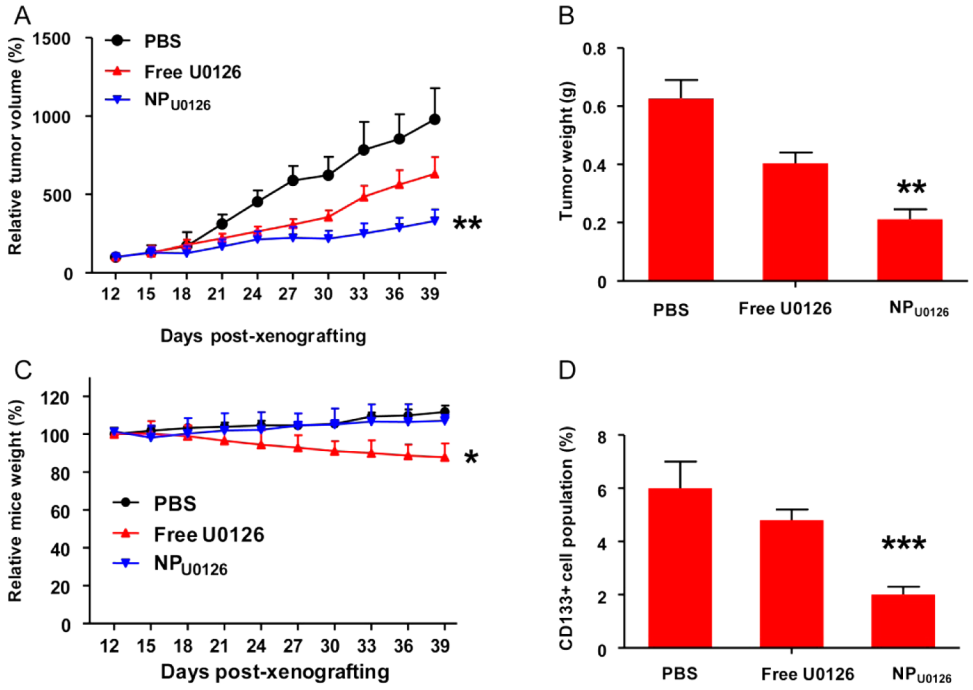

Figure 6. (A)Tumor growth curve, (B) tumor weight, and (C) body weight change of HepG2 xenograft tumor model after treating with free U0126 or NP$_{U0126}$ at 10 mg/kg. (D) Proportion of CSCs after the last treatment was analyzed by FACS. Data are shown as means ± SD (n = 5). (*) p < 0.05, (**) p < 0.01, (***) p < 0.001, NP$_{U0126}$ compared with free U0126.

observed in the Hep3B and SMMC7721 mammosphere cells. Also, the CSC populations (CD133 positive) of HCC after different formulation treatments were analyzed by FACS, as shown in Figure 4B. The nanoparticles' encapsulation could augment the CSC inhibition ability of U0126, which was consistent with the results of the sphere formation assay. Moreover, the in vitro limiting dilution assays (LDA) were performed with HCC mammosphere cells after NP$_{U0126}$ or free U0126 treatment. As shown in Figure 4C, the CSC frequency of HCC mammosphere cells could be decreased by U0126, and the drug-loaded nanoparticles could reduce the frequency of CSCs more significantly.

Biodistribution of Drug Encapsulated Nanoparticles in Vivo. Nanoparticle-mediated therapeutics have been demonstrated to enhance anticancer effects compared with the small-molecule therapeutic agents, attributed to overcoming the limitations of the therapeutic agents via the longer circulation half-lives, improved pharmacokinetics and highly specific tumor site enrichment.[56] Herein, we investigated whether U0126-loaded nanoparticles could prolong the circulation half-life and enhance the delivery of U0126 into the engrafted tumors. The U0126 concentrations in plasma versus time are shown in Figure 5A. The fact that free U0126 is rapidly eliminated following injection is consistent with previous reports. However, drug-loaded nanoparticles showed significantly slower clearance than free drugs. The U0126 circulation half-lives (t1/2z) of NP$_{U0126}$ and free U0126 were calculated by DAS 2.0 software to be 10.02 and 4.04 h, respectively. More importantly, NP$_{U0126}$ also showed a higher area under the concentration curve (AUC), which was 10.5-fold greater than free U0126.

The nanoparticles possessing a PEG protection layer is believed to be beneficial for their accumulation in tumor sites through the EPR effect. To demonstrate this, we administered U0126 encapsulated the nanoparticles and free U0126 by iv injection to HepG2 tumor model and detected drug content in the tumor issues and major organs by HPLC. As shown in Figure 5B, the U0126 level in the tumor tissue was 2.69 ± 0.38

DOI: 10.1021/am508262j
ACS Appl. Mater. Interfaces 2015, 7, 1012−1020

μg/g for mice receiving a single injection of drug-loaded nanoparticles, while the corresponding levels for mice treated with free U0126 was only 0.79 ± 0.18 ng/g. This demonstrated that the drug-loaded nanoparticles can enhance the accumulation of U0126 in HCC tumors, due to the EPR effect.

Tumor Growth Inhibition Mediated by Systemic Delivery of NP_{U0126}. To further verify whether the delivery system (NP_{U0126}) could effectively inhibit tumor growth and inhibit CSCs following systemic administration, we treated HepG2 xenograft-bearing mice with NP_{U0126} or free U0126 through iv injection twice a week. As shown in Figure 6A, free U0126 (10 mg/kg) moderately inhibited the tumor growth, while U0126 encapsulated with nanoparticles reduced tumor growth prominently. At the end of the treatment, the tumor weight was analyzed (Figure 6B), which supported the results of tumor suppression. It should be mentioned that when free U0126 inhibited the tumor growth, the body weight of mouse HepG2 xenograft significantly decreased (Figure 6C). Moreover, the AST, ALT, and LDH level of the serum after free U0126 treatment obviously increased (Figure S2, Supporting Information), implying free the small molecular inhibitor might induce significant side effects during treatments. On the contrary, systemic administration of NP_{U0126} showed little effect on the mice's body weight and liver damage-related cytokines in both tumor models, suggesting that the formulation of the drug-loaded nanoparticles would potentially be safer for HCC cancer therapy than the free U0126.

Subsequently, to investigate whether NP_{U0126} could inhibit the bulk cancer cells and CSCs simultaneously, we examined the population of CSCs (CD133 positive) recovered from the tumors at the end of the treatments. As shown in Figure 6D, the percentage of CSCs from tumor cells treated with U0126 (4.8%) was slightly lower than that of PBS control (6%). When treated with NP_{U0126}, the CSC ratio (2%) was significantly reduced, which was consistent with the tumor inhibition effect.

Cell proliferation in the tumor tissue after treatment was analyzed by PCNA. As shown in Figure 7, a reduced number of PCNA-positive tumoral cells (brown) in tumor tissue are observed after treatment with free U0126 compared with PBS treatment. Moreover, nanoparticles carrying U0126 was more effective in inhibiting tumor proliferation than free U0126. Cell apoptosis in the tumor tissue after treatments was detected using TUNEL assay. Corresponding with the tumor growth inhibition, treatment with NP_{U0126} increased the TUNEL-positive tumoral cells (green) than free U0126 treatment.

CONCLUSION

The PEG-PLA-based single-emulsion technique was exploited for the dual functional MEK/ERK inhibitor encapsulation (NP_{U0126}). The nanoparticle delivery system could enhance the cellular uptake of U0126 in drug-resistant HCC CSCs and augment the cytotoxicity of the U0126 compared to using free drugs. Moreover, the nanoparticles' encapsulation increased the self-renewal capability inhibition of U0126. In addition, a prolonged circulation time and enhanced tumor accumulation were achieved by U0126-loaded nanoparticles. Systemic delivery of NP_{U0126} significantly inhibits both tumor growth and the CSC population in mice bearing HepG2 xenografts. Importantly, the delivery of U0126 by this nanoparticle system does not cause in vivo systemic toxicity, providing a novel approach for HCC therapy.

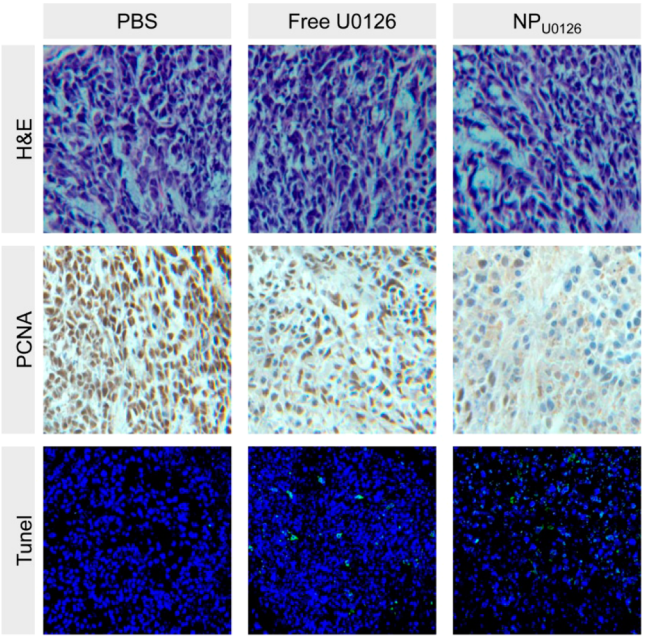

Figure 7. H&E, PCNA, and TUNEL analyses of tumor tissues after treatment with different formulations; (brown) PCNA-positive proliferating cells and (green) TUNEL-positive apoptotic cells.

ASSOCIATED CONTENT

Supporting Information

Cytotoxicity of free PEG_{5K}-PLA_{11K} nanoparticles and mouse serum cytokines change after animal study. This material is available free of charge via the Internet at http://pubs.acs.org.

AUTHOR INFORMATION

Corresponding Author

*Tel.: +86 551 63600335. Fax: +86 551 63600402. E-mail: jwang699@ustc.edu.cn.

Notes

The authors declare no competing financial interest.

ACKNOWLEDGMENTS

This work was supported by the National Basic Research Program of China (973 Programs, 2012CB932500, 2015CB932100), and the National Natural Science Foundation of China (51125012, 31470965, 51390482).

REFERENCES

(1) Avila, M. A.; Berasain, C.; Sangro, B.; Prieto, J. New Therapies for Hepatocellular Carcinoma. *Oncogene* **2006**, *25*, 3866−3884.

(2) Llovet, J. M.; Bruix, J. Novel Advancements in the Management of Hepatocellular Carcinoma in 2008. *J. Hepatol.* **2008**, *48*, S20−S37.

(3) Aravalli, R. N.; Steer, C. J. Cressman, ENK. Molecular Mechanisms of Hepatocellular Carcinoma. *Hepatology* **2008**, *48*, 2047−2063.

(4) Haraguchi, N.; Ishii, H.; Mimori, K.; Tanaka, F.; Ohkuma, M.; Kim, H. M.; Akita, H.; Takiuchi, D.; Hatano, H.; Nagano, H.; Barnard, G. F.; Doki, Y.; Mori, M. CD13 is a Therapeutic Target in Human Liver Cancer Stem Cells. *J. Clin. Invest.* **2010**, *120*, 3326−3339.

(5) Chen, X.; Lingala, S.; Khoobyari, S.; Nolta, J.; Zern, M. A.; Wu, J. Epithelial Mesenchymal Transition and Hedgehog Signaling Activation are Associated with Chemoresistance and Invasion of Hepatoma Subpopulations. *J. Hepatol.* **2011**, *55*, 838−845.

(6) Bodzin, A. S.; Wei, Z.; Hurtt, R.; Gu, T.; Doria, C. Gefitinib Resistance in HCC Mahlavu Cells: Upregulation of CD133

DOI: 10.1021/am508262j
ACS Appl. Mater. Interfaces 2015, 7, 1012−1020

Expression, Activation of IGF-1R Signaling Pathway, and Enhancement of IGF-1R Nuclear Translocation. *J. Cell. Physiol.* **2012**, *227*, 2947−2952.
(7) Piao, L. S.; Hur, W.; Kim, T. K.; Hong, S. W.; Kim, S. W.; Choi, J. E.; Sung, P. S.; Song, M. J.; Lee, B. C.; Hwang, D.; Yoon, S. K. CD133(+) Liver Cancer Stem Cells Modulate Radioresistance in Human Hepatocellular Carcinoma. *Cancer Lett.* **2012**, *315*, 129−137.
(8) Suetsugi, A.; Nagaki, M.; Aoki, H.; Motohashi, T.; Kunisada, T.; Moriwaki, H. Characterization of CD133(+) Hepatocellular Carcinoma Cells as Cancer Stem/Progenitor Cells. *Biochem. Biophys. Res. Commun.* **2006**, *351*, 820−824.
(9) Yin, S.; Li, J.; Hu, C.; Chen, X.; Yao, M.; Yan, M.; Jiang, G.; Ge, C.; Xie, H.; Wan, D.; Yang, S.; Zheng, S.; Gu, J. CD133 Positive Hepatocellular Carcinoma Cells Possess High Capacity for Tumorigenicity. *Int. J. Cancer* **2007**, *120*, 1444−1450.
(10) Ma, S.; Tang, K. H.; Chan, Y. P.; Lee, T. K.; Kwan, P. S.; Castilho, A.; Ng, I.; Man, K.; Wong, N.; To, K. F.; Zheng, B. J.; Lai, P. B.; Lo, C. M.; Chan, K. W.; Guan, X. Y. Mir-130b Promotes Cd133(+) Liver Tumor-Initiating Cell Growth and Self-Renewal Via Tumor Protein 53-Induced Nuclear Protein 1. *Cell Stem Cell* **2010**, *7*, 694−707.
(11) Kim, H.; Choi, G. H.; Na, D. C.; Ahn, E. Y.; IIKim, G.; Lee, J. E.; Cho, J. Y.; Yoo, J. E.; Choi, J. S.; Park, Y. N. Human Hepatocellular Carcinomas with "Stemness"-Related Marker Expression: Keratin 19 Expression and a Poor Prognosis. *Hepatology* **2011**, *54*, 1707−1717.
(12) Sun, Y. F.; Xu, Y.; Yang, X. R.; Guo, W.; Zhang, X.; Qiu, S. J.; Shi, R. Y.; Hu, B.; Zhou, J.; Fan, J. Circulating Stem Cell-Like Epithelial Cell Adhesion Molecule-Positive Tumor Cells Indicate Poor Prognosis of Hepatocellular Carcinoma after Curative Resection. *Hepatology* **2013**, *57*, 1458−1468.
(13) Sun, T. M.; Wang, Y. C.; Wang, F.; Du, J. Z.; Mao, C. Q.; Sun, C. Y.; Tang, R. Z.; Liu, Y.; Zhu, J.; Zhu, Y. H.; Yang, X. Z.; Wang, J. Cancer Stem Cell Therapy Using Doxorubicin Conjugated to Gold Nanoparticles via Hydrazone Bonds. *Biomaterials* **2014**, *35*, 836−845.
(14) Ke, X. Y.; Ng, V. W. L.; Gao, S. J.; Tong, Y. W.; Hedrick, J. L.; Yang, Y. Y. Co-Delivery of Thioridazine and Doxorubicin Using Polymeric Micelles for Targeting Both Cancer Cells and Cancer Stem Cells. *Biomaterials* **2014**, *35*, 1096−1108.
(15) Li, R. J.; Ying, X.; Zhang, Yan.; Ju, R. J.; Wang, X. X.; Yao, H. J.; Men, Y.; Tian, W.; Yu, Y.; Zhang, L.; Huang, R. J.; Lu, W. L. All-Trans Retinoic Acid Stealth Liposomes Prevent the Relapse of Breast Cancer Arising from the Cancer Stem Cells. *J. Controlled Release* **2011**, *49*, 281−291.
(16) Zhou, Y.; Yang, J.; Rhim, J. S.; Kopecek, J. HPMA Copolymer-Based Combination Therapy Toxic to Both Prostate Cancer Stem/Progenitor Cells and Differentiated Cells Induces Durable Anti-Tumor Effects. *J. Controlled Release* **2013**, *172*, 946−953.
(17) Zhao, W.; Wang, L.; Han, H.; Jin, K.; Lin, N.; Guo, T.; Chen, Y. D.; Cheng, H. P.; Lu, F. M.; Fang, W. G. 1b50−1, a mAb Raised against Recurrent Tumor Cells, Targets Liver Tumor-Initiating Cells by Binding to the Calcium Channel $\alpha 2\delta 1$ Subunit. *Cancer Cell* **2013**, *23*, 541−556.
(18) Lewis, T. S.; Shapiro, P. S.; Ahn, N. G. Signal Transduction through MAP Kinase Cascades. *Adv. Cancer Res.* **1998**, *74*, 49−139.
(19) Ballif, B. A.; Blenis, J. Molecular Mechanisms Mediating Mammalian Mitogen-Activated Protein Kinase (MAPK) Kinase (MEK)-Mapk Cell Survival Signals. *Cell Growth Differ.* **2001**, *12*, 397−408.
(20) Krueger, J. S.; Keshamouni, V. G.; Atanaskova, N.; Reddy, K. B. Temporal and Quantitative Regulation of Mitogen-Activated Protein Kinase (MAPK) Modulates Cell Motility and Invasion. *Oncogene* **2001**, *20*, 4209−4218.
(21) Cowley, S.; Paterson, H.; Kemp, P.; Marshall, C. J. Activation of MAP Kinase Kinase Is Necessary and Sufficient for PC12 Differentiation and for Transformation of NIH 3T3 Cells. *Cell* **1994**, *77*, 841−852.
(22) Mansour, S. J.; Matten, W. T.; Hermann, A. S.; Candia, J. M.; Rong, S.; Fukasawa, K.; Vande Woude, G. F.; Ahn, N. G. Transformation of Mammalian Cells by Constitutively Active MAP Kinase Kinase. *Science* **1994**, *265*, 966−970.
(23) Wiesenauer, C. A.; Yip-Schneider, M. T.; Wang, Y. F.; Schmidt, C. M. Multiple Anticancer Effects of Blocking MEK-ERK Signaling in Hepatocellular Carcinoma. *J. Am. Coll. Surg.* **2004**, *198*, 410−421.
(24) Yip, N. C.; Fombon, I. S.; Liu, P.; Brown, S.; Kannappan, V.; Armesilla, A. L.; Xu, B.; Cassidy, J.; Darling, J. L.; Wang, W. Disulfiram Modulated ROS-MAPK and NfκB Pathways and Targeted Breast Cancer Cells with Cancer Stem Cell-Like Properties. *Br. J. Cancer* **2011**, *104*, 1564−1574.
(25) Dong, Y. C.; Han, Q. L.; Zou, Y.; Deng, Z. L.; Lu, X. L.; Wang, X. H.; Zhang, W. H.; Jin, H.; Su, J.; Jiang, T.; Ren, H. Long-Term Exposure to Imatinib Reduced Cancer Stem Cell Ability through Induction of Cell Differentiation via Activation of MAPK Signaling in Glioblastoma Cells. *Mol. Cell. Biochem.* **2012**, *370*, 89−102.
(26) Ma, L. Y.; Shan, Y.; Bai, R.; Xue, L. T.; Eide, C. A.; Ou, J. H.; Zhu, L. H. J.; Hutchinson, L.; Cerny, J.; Khoury, H. J.; Sheng, Z.; Druker, B. J.; Li, S. G.; Green, M. R. A Therapeutically Targetable Mechanism of Bcr-Abl-Independent Imatinib Resistance in Chronic Myeloid Leukemia. *Sci. Transl. Med.* **2014**, *6*, 252.
(27) Favata, M. F.; Horiuchi, K. Y.; Manos, E. J.; Daulerio, A. J.; Stradley, D. A.; Feeser, W. S.; Van Dyk, D. E.; Pitts, W. J.; Earl, R. A.; Hobbs, F.; Copeland, R. A.; Magolda, R. L.; Scherle, P. A.; Trzaskos, J. M. Identification of a Novel Inhibitor of Mitogen-Activated Protein Kinase Kinase. *J. Biol. Chem.* **1998**, *273*, 18623−18632.
(28) Ferrari, M. Frontiers in Cancer Nanomedicine: Directing Mass Transport through Biological Barriers. *Trends Biotechnol.* **2010**, *28*, 181−188.
(29) Florence, A. T. "Targeting" Nanoparticles: The Constraints of Physical Laws and Physical Barriers. *J. Controlled Release* **2012**, *164*, 115−124.
(30) Chrastina, A.; Massey, K. A.; Schnitzer, J. E. Overcoming in Vivo Barriers to Targeted Nanodelivery. *Wiley Interdiscip. Rev.: Nanomed. Nanobiotechnol.* **2011**, *3*, 421−437.
(31) Cabral, H.; Matsumoto, Y.; Mizuno, K.; Chen, Q.; Murakami, M.; Kimura, M.; Terada, Y.; Kano, M. R.; Miyazono, K.; Uesaka, M.; Nishiyama, N.; Kataoka, K. Accumulation of Sub-100 nm Polymeric Micelles in Poorly Permeable Tumours Depends on Size. *Nat. Nanotechnol.* **2011**, *6*, 815−823.
(32) Davis, M. E.; Chen, Z.; Shin, D. M. Nanoparticle Therapeutics: An Emerging Treatment Modality for Cancer. *Nat. Rev. Drug Discovery* **2008**, *7*, 771−782.
(33) Peer, D.; Karp, J. M.; Hong, S.; Farokhzad, O. C.; Margalit, R.; Langer, R. Nanocarriers as an Emerging Platform for Cancer Therapy. *Nat. Nanotechnol.* **2007**, *2*, 751−760.
(34) Heidel, J. D.; Davis, M. E. Clinical Developments in Nanotechnology for Cancer Therapy. *Pharm. Res.* **2011**, *28*, 187−199.
(35) Matsumura, Y.; Maeda, H. A New Concept for Macromolecular Therapeutics in Cancer-Chemotherapy-Mechanism of Tumoritropic Accumulation of Proteins and the Antitumor Agent Smancs. *Cancer Res.* **1986**, *46*, 6387−6392.
(36) Yuan, Y. Y.; Mao, C. Q.; Du, X. J.; Du, J. Z.; Wang, F.; Wang, J. Surface Charge Switchable Nanoparticles Based on Zwitterionic Polymer for Enhanced Drug Delivery to Tumor. *Adv. Mater.* **2012**, *24*, 5476−5480.
(37) Yang, X. Z.; Du, X. J.; Liu, Y.; Zhu, Y. H.; Liu, Y. Z.; Li, Y. P.; Wang, J. Rational Design of Polyion Complex Nanoparticles to Overcome Cisplatin Resistance in Cancer Therapy. *Adv. Mater.* **2014**, *26*, 931−936.
(38) Lai, M. H.; Lee, S.; Smith, C. E.; Kim, K.; Kong, H. Tailoring Polymersome Bilayer Permeability Improves Enhanced Permeability and Retention Effect for Bioimaging. *ACS Appl. Mater. Interfaces* **2014**, *6*, 10821−10829.
(39) Wang, S.; Zhang, S. N.; Liu, J. Q.; Liu, Z. Y.; Su, L.; Wang, H. J.; Chang, J. pH- and Reduction-Responsive Polymeric Lipid Vesicles for Enhanced Tumor Cellular Internalization and Triggered Drug Release. *ACS Appl. Mater. Interfaces* **2014**, *6*, 10706−10713.
(40) Li, K.; Wang, S. G.; Wen, S. H.; Tang, Y. Q.; Li, J. P.; Shi, X. Y.; Zhao, Q. H. Enhanced in Vivo Antitumor Efficacy of Doxorubicin

DOI: 10.1021/am508262j
ACS Appl. Mater. Interfaces 2015, 7, 1012−1020

Encapsulated within Laponite Nanodisks. *ACS Appl. Mater. Interfaces* **2014**, *6*, 12328−12334.
(41) Ma, Y. C.; Wang, J. X.; Tao, W.; Qian, H. S.; Yang, X. Z. Polyphosphoester-Based Nanoparticles with Viscous Flow Core Enhanced Therapeutic Efficacy by Improved Intracellular Drug Release. *ACS Appl. Mater. Interfaces* **2014**, *6*, 16174−16181.
(42) Cheng, Y.; Yu, S. L.; Zhen, X.; Wang, X.; Wu, W.; Jiang, X. Q. Alginic Acid Nanoparticles Prepared through Counterion Complexation Method as a Drug Delivery System. *ACS Appl. Mater. Interfaces* **2012**, *4*, 5325−5332.
(43) Quan, L.; Liu, S.; Sun, T. T.; Guan, X. G.; Lin, W. H.; Xie, Z. G.; Huang, Y. B.; Wang, Y. Q.; Jing, X. B. Near-Infrared Emitting Fluorescent BODIPY Nanovesicles for in Vivo Molecular Imaging and Drug Delivery. *ACS Appl. Mater. Interfaces* **2014**, *6*, 16166−16173.
(44) Wang, D.; Huang, J.; Wang, X.; Yu, Y.; Zhang, H.; Chen, Y.; Liu, J.; Sun, Z.; Zou, H.; Sun, D.; Zhou, G.; Zhang, G.; Lu, Y.; Zhong, Y. The Eradication of Breast Cancer Cells and Stem Cells by 8-Hydroxyquinoline-Loaded Hyaluronan Modified Mesoporous Silica Nanoparticle-Supported Lipid Bilayers Containing Docetaxel. *Biomaterials* **2013**, *34*, 7662−7673.
(45) Liu, Y.; Lu, W. L.; Guo, J.; Du, J.; Li, T.; Wu, J. W.; Wang, G. L.; Wang, J. C.; Zhang, X.; Zhang, Q. A Potential Target Associated with Both Cancer and Cancer Stem Cells: A Combination Therapy for Eradication of Breast Cancer Using Vinorelbine Stealthy Liposomes Plus Parthenolide Stealthy Liposomes. *J. Controlled Release* **2008**, *129*, 18−25.
(46) Yang, X. Z.; Dou, S.; Sun, T. M.; Mao, C. Q.; Wang, H. X.; Wang, J. Systemic Delivery of siRNA with Cationic Lipid Assisted PEG-PLA Nanoparticles for Cancer Therapy. *J. Controlled Release* **2011**, *156*, 203−211.
(47) Hu, Y.; Smyth, G. K. ELDA: Extreme Limiting Dilution Analysis for Comparing Depleted and Enriched Populations in Stem Cell and Other Assays. *J. Immunol. Methods* **2009**, *347*, 70−78.
(48) Sun, C. Y.; Dou, S.; Du, J. Z.; Yang, X. Z.; Li, Y. P.; Wang, J. Doxorubicin Conjugate of Poly(ethylene glycol)-Block Polyphosphoester for Cancer Therapy. *Adv. Healthcare Mater.* **2014**, *3*, 261−272.
(49) Sun, T. M.; Du, J. Z.; Yao, Y. D.; Mao, C. Q.; Dou, S.; Huang, S. Y.; Zhang, P. Z.; Leong, K. W.; Song, E. W.; Wang, J. Simultaneous Delivery of siRNA and Paclitaxel via a "Two-in-One" Micelleplex Promotes Synergistic Tumor Suppression. *ACS Nano* **2011**, *5*, 1483−1494.
(50) Liu, Y.; Zhu, Y. H.; Mao, C. Q.; Dou, S.; Shen, S.; Tan, Z. B.; Wang, J. Triple Negative Breast Cancer Therapy with CDK1 siRNA Delivered by Cationic Lipid Assisted PEG-PLA Nanoparticles. *J. Controlled Release* **2014**, *192*, 114−121.
(51) Merisko-Liversidge, E.; Liversidge, G. G.; Cooper, E. R. Nanosizing: A Formulation Approach for Poorly-Water-Soluble Compounds. *Eur. J. Pharm. Sci.* **2003**, *18*, 113−120.
(52) Doi, K.; Oku, N.; Toyota, T.; Shuto, S.; Sakai, A.; Itoh, H.; Okada, S. Therapeutic Effect of Reticuloendothelial System (RES)-Avoiding Liposomes Containing a Phospholipid Analogue of 5-Fluorouracil, Dipalmitoylphosphatidylfluorouridine, in Meth Asarcoma-Bearing Mice. *Biol. Pharm. Bull.* **1994**, *17*, 1414−1416.
(53) Merisko-Liversidge, E. M.; Liversidge, G. G. Drug Nanoparticles: Formulating Poorly Water-Soluble Compounds. *Toxicol. Pathol.* **2008**, *36*, 43−48.
(54) Larson, T. A.; Joshi, P. R.; Sokolov, K. Preventing Protein Adsorption and Macrophage Uptake of Gold Nanoparticles via a Hydrophobic Shield. *ACS Nano* **2012**, *6*, 9182−9190.
(55) Cao, L.; Zhou, Y.; Zhai, B.; Liao, J.; Xu, W.; Zhang, R. X.; Li, J.; Zhang, Y.; Chen, L.; Qian, H. H.; Wu, M. C.; Yin, Z. F. Sphere-Forming Cell Subpopulations with Cancer Stem Cell Properties in Human Hepatoma Cell Lines. *BMC Gastroenterol.* **2011**, *11*, 71.
(56) Ernsting, M. J.; Murakami, M.; Roy, A.; Li, S. D. Factors Controlling the Pharmacokinetics, Biodistribution and Intratumoral Penetration of Nanoparticles. *J. Controlled Release* **2013**, *172*, 782−794.

DOI: 10.1021/am508262j
ACS Appl. Mater. Interfaces 2015, 7, 1012−1020